How to cite: *Angew. Chem. Int. Ed.* **2023**, *62*, e202309838
doi.org/10.1002/anie.202309838

Antiviral Agents

Synthetic Heparanase Inhibitors Can Prevent Herpes Simplex Viral Spread

Pradeep Chopra[+], Tejabhiram Yadavalli[+], Francesco Palmieri, Seino A. K. Jongkees, Luca Unione, Deepak Shukla, and Geert-Jan Boons**

Abstract: Herpes simplex virus (HSV-1) employs heparan sulfate (HS) as receptor for cell attachment and entry. During late-stage infection, the virus induces the upregulation of human heparanase (Hpse) to remove cell surface HS allowing viral spread. We hypothesized that inhibition of Hpse will prevent viral release thereby representing a new therapeutic strategy for HSV-1. A range of HS-oligosaccharides was prepared to examine the importance of chain length and 2-*O*-sulfation of iduronic moieties for Hpse inhibition. It was found that hexa- and octasaccharides potently inhibited the enzyme and that 2-*O*-sulfation of iduronic acid is tolerated. Computational studies provided a rationale for the observed structure–activity relationship. Treatment of human corneal epithelial cells (HCEs) infected with HSV-1 with the hexa- and octasaccharide blocked viral induced shedding of HS which significantly reduced spread of virions. The compounds also inhibited migration and proliferation of immortalized HCEs thereby providing additional therapeutic properties.

Introduction

Human heparanase (Hpse) is an endo-β-D-glucuronidase that orchestrates the remodelling of extracellular matrix (ECM) and basement membrane by hydrolysing heparan sulfate proteoglycans (HSPGs),[1] which are protein-anchored anionic polysaccharides of alternating glucosamine (GlcN) and uronic acids (glucuronic acid, GlcA or iduronic acid, IdoA) with varying levels of sulfation.[2] The substrate specificity of Hpse is rather broad and primarily defined by the pattern of sulfation around a potential cleavage site and appropriate substrates are thought to be at the border of highly sulfated and lesser sulfated regions.[3] Cleavage of HS chains results in the release of sequestered growth factors, cytokines, and lipoproteins thereby mediating many biological processes.[4] Hpse has been implicated in various diseases such as tumour metastasis, type-1 diabetes, renal fibrosis, and inflammation.[5] As a result, the development of Hpse inhibitors has received considerable attention and various approaches are being pursued such as modified heparins, sulfated oligosaccharides, small molecules and anti-Hpse antibodies.[6]

Hpse also regulates the lifecycle of many human viruses such as dengue virus (DENV), human papilloma virus (HPV), respiratory syncytial virus (RSV), adenovirus (ADNV), hepatitis C virus (HCV) and herpes simplex virus (HSV).[7] HSV is an enveloped double-stranded DNA virus that belongs to alpha-herpesvirus subfamily.[8] HSV type-1 is a major cause of corneal keratitis and encephalitis, which when left untreated can result in the loss of vision, neurological deficits, seizures or even death.[9] Although acyclovir and derivatives thereof can treat active herpes infections, these drugs do not stop permanent viral latency, allowing the virus to reactivate and cause clinical disease at a later point in time.[10] Therefore, there is a need to develop therapeutic strategies that target other key steps in the viral lifecycle such as entry and spread to other cells and tissues.

[*] Dr. P. Chopra,[+] Prof. Dr. G.-J. Boons
Complex Carbohydrate Research Center, University of Georgia
Athens, GA 30602 (USA)
E-mail: gjboons@cccrc.uga.edu
Dr. T. Yadavalli,[+] Prof. Dr. D. Shukla
Department of Ophthalmology and Visual Sciences, University of Illinois at Chicago
Chicago, IL 60612 (USA)
E-mail: dshukla@uic.edu
F. Palmieri, Dr. S. A. K. Jongkees, Dr. L. Unione, Prof. Dr. G.-J. Boons
Department of Chemical Biology and Drug Discovery, Utrecht Institute for Pharmaceutical Sciences, Utrecht University
3584 CG Utrecht (The Netherlands)
E-mail: g.j.p.h.boons@uu.nl
Dr. L. Unione
Current address: CICbioGUNE, Basque Research & Technology Alliance (BRTA)
Bizkaia Technology Park, 48160 Derio, Bizkaia, (Spain)
Prof. Dr. G.-J. Boons
Bijvoet Center for Biomolecular Research, Utrecht University
3584 CG Utrecht (The Netherlands)
and
Department of Chemistry, University of Georgia
Athens, GA 30602 (USA)
[+] These authors contributed equally to this work.

HSV-1 uses cell surface HSPGs of host cells as co-receptor.[11] Infection is initiated by attachment of viral glycoprotein B (gB) and gC to cell surface HSPGs. Next, gD, engages with one of its receptors, nectin-1, herpes virus entry mediator (HVEM) or 3-*O*-sulfated HS, resulting in a conformational change.[12] Activated gD binds to a heterodimer of the glycoproteins, gH and gL, resulting in cell penetration and capsid release. After replication, HSV-1 leaves host cells and spreads to other uninfected cells, which is facilitated by viral glycoprotein heterodimer, gE/gI redistribution to cell junctions. At these tight and adherent junctions, the virus utilizes gE/gI to attach to its receptors that support lateral spread from infected to uninfected cells. HSV can also produce fusion pores at these junctions to egress or be released into the ECM.[13]

Previously, we described that HSV-1 has a remarkable ability to modulate HS biosynthesis for optimal infection and viral spread.[14] During the initial stage of infection, cellular HS biosynthesis is upregulated enhancing viral attachment and cell entry. In later stages of infection, the expression of Hpse is upregulated ensuring that HSPG's are cleaved resulting in the detachment of the virus.[7,13b] We anticipated that inhibition of Hpse may prevent viral release and may represent a therapeutic strategy for HSV-1 and other viruses that rely on Hpse for infection.

In this study, we designed and synthesized differently sulfated di-, tetra-, hexa- and octasaccharides and evaluated their ability to inhibit Hpse activity by a colorimetric[15] and homogeneous time-resolved fluorescence (HTRF)[16] assay. It was found that increasing the chain length of the HS oligosaccharides results in more potent inhibition, and it revealed that 2-*O*-sulfation of IdoA is tolerated by the enzyme. Molecular modeling studies provided a rationale for the observed structure–activity relationship (SAR). Treatment of human corneal epithelial cells (HCEs) infected with HSV-1 with the hexa- and octasaccharide blocked viral induced shedding of HS which in turn resulted in a significant reduction of shedded virions. The compounds also inhibited migration and proliferation of immortalized HCEs thereby providing additional therapeutic properties.

Results and Discussion

Design and chemical synthesis of well-defined HS oligosaccharides as inhibitors of Hpse

Hpse is a retaining endoglycosidase that cleaves GlcA-GlcNS linkages of polymeric HS.[17] A crystal structure of Hpse in complex with a tetrasaccharide has provided a structural rationale for the catalytic mechanism and substrate recognition by this enzyme.[18] It has a large cleft in which residues Glu343 and Glu225 function as catalytic nucleophile and acid-base required for a retaining catalytic cleavage mechanism. Furthermore, the binding cleft is lined with basic amino acids (Lys159, Lys161, Lys231, Arg272, Arg273, Lys274 and Arg303) important for binding of negative charged HS chains. The sulfates of GlcNS(6S) at the −2 subsite and GlcNS6S at the +1 subsite make ionic interactions with side chains of basic amino acid in the binding cleft. Previous inhibition studies with differently sulfated trisaccharides had already indicated the importance of these sulfates for substrate recognition.[19] The co-crystal structure showed that IdoA at the −1 subsite, where glycosidic bond cleavage takes place, adopts a $^{2}S_{O}$ conformation. However, in this configuration the catalytic nucleophile and acid-base are not properly positioned for glycosidic bond cleavage making IdoA-containing compounds resistant to Hspe cleavage. The X-ray structures also indicated that GlcUA(2S) or IdoUA(2S) cannot be accommodated at the −1 subsite because of steric clashes between the 2-*O*-sulfate and Asn224.[18] We examined the binding cleft of Hpse (apo-structure PDB: 5E8M),[18] which is 30 Å in length, and anticipated that it can accommodate oligosaccharides as large as an octasaccharide. Therefore, we expected that IdoA containing HS-oligosaccharides of increasing chain length will provide increasingly potent inhibitors. It is known that glycol split heparins, in which vicinal diols have been oxidized by sodium periodate followed reduction of the resulting aldehydes by sodium borohydride to alcohols, can potently inhibit Hpse.[20] This oxidation affects mainly non-sulfated glucuronic and iduronic acid residues, and as a result glycol split heparin contains mainly IdoA2S moieties.[21] Thus, these observations indicate that Hpse can accommodate IdoA2S residues. Based on these findings, we were compelled to synthesize HS oligosaccharides **1**–**6** (Figure 1D) and probe their inhibitory potential for Hpse. Compounds **1**–**4** were designed to probe the influence of C-2 sulfation of IdoA on inhibitory activity and compounds **5** and **6** to examine the importance of oligosaccharide length. Compounds **1**–**6** were prepared by a modular synthetic approach utilizing a set of disaccharide building blocks that mimic sulfated disaccharide moieties in HS.[22] At an appropriate stage of synthesis, levulinoyl (Lev) esters can selectively be removed to provide alcohols for sulfation.

The preparation of hexasaccharide **5** is described in Scheme 1. Thus, a triflic acid (TfOH) mediated glycosylation of glycosyl acceptor **7** with donor **8** yielded tetrassacharide **9** as only the α-anomer. The anomeric configuration was confirmed by the $^{3}J_{H1,H2}$ coupling constant (3.9 Hz) and ^{13}C chemical shifts of C-1 (97.7 ppm) (see *Supporting Information*). The fluorenylmethyloxycarbonate (Fmoc) group of **9** was removed by triethylamine (Et_3N) in dichloromethane to give tetrasaccharide acceptor **10** that was glycosylated with disaccharide donor **11** to obtain hexassacharide **12** as only the α-anomer. The Lev esters were removed by treatment with hydrazine acetate and the resulting alcohols were sulfated by previously optimized conditions employing sulfur trioxide-triethylamine complex ($SO_3.NEt_3$) at elevated temperature (60 °C) for a prolonged reaction time (16 h).[23] However, under these conditions, the Fmoc protection group was removed and the resulting alcohol get sulfated. To avoid oversulfation, the Fmoc of **12** was replaced by an acetyl ester to give **13** by removal of Fmoc by Et_3N in dichloromethane followed by acetylation of the resulting hydroxyl by acetic anhydride in pyridine in the presence of a catalytic amount of 4-dimethylaminopyridine (DMAP). The Lev esters of **13** were removed by treatment with hydrazine

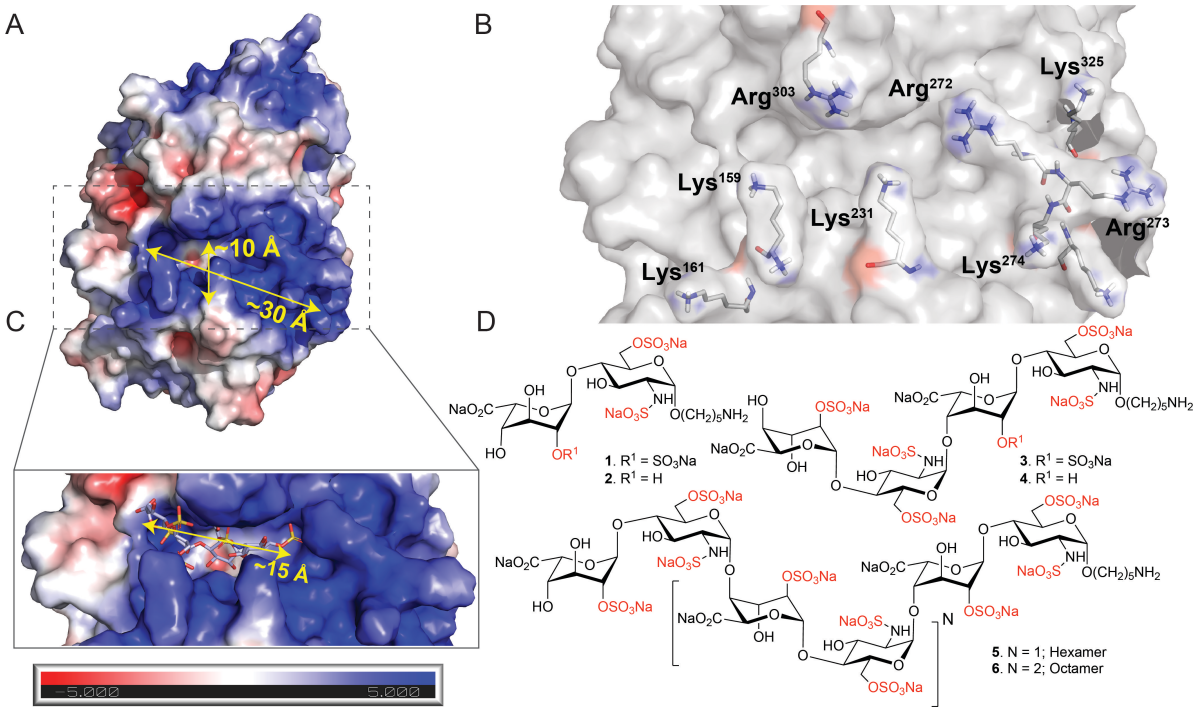

Figure 1. Rational design of inhibitor of human heparanase (Hpse). (A) Surface representation of Hpse enzyme; (B) Details of the positively charged residues composing the substrate binding cleft; (C) Surface and stick representation of GlcNS-GlcA-GlcNS-GlcA-pNP bound to Hpse; (D) Chemical structure of target compounds **1**–**6**.

acetate, and the resulting alcohols were selectively sulfated using SO_3.NEt_3 in dimethylformamide (DMF) at 60 °C. Next, the methyl esters were saponified by first treatment with hydrogen peroxide (H_2O_2) and lithium hydroxide (LiOH) in tetrahydrofuran (THF) followed by saponification of the other esters using sodium hydroxide (NaOH) in methanol (MeOH) to give **14**. Under Staudinger conditions using trimethylphosphine (PMe_3) and NaOH, the azides of **14** were reduced to amines, which were *N*-sulfated employing sulfur trioxide-pyridine complex (SO_3.Py) in MeOH in the presence of Et_3N and NaOH to provide **15**. Finally, the target hexasaccharide **5** was obtained by global deprotection of **15** involving two-step hydrogenation by first using palladium on carbon (Pd/C) in a mixture of *tert*-butanol/water (*t*BuOH/H_2O) to cleave the protecting group of the anomeric linker, and then over palladium hydroxide on carbon ($Pd(OH)_2$/C) to remove the benzyl and naphthylmethyl ethers. The compound was purified by size exclusion column chromatography over a Biogel P-2 and followed by Na^+ exchange using Dowex [Na^+] resin. HS oligosaccharides **1**–**4** and **6** were prepared in a similar manner as detailed in *Supporting Information* (Schemes S1–S3). The target compounds **1**–**6** were obtained in quantities ranging from 5 to 10 mg and fully characterized by high-resolution electrospray ionization-mass spectrometry (ESI-MS) and nuclear magnetic resonance (NMR). ^{1}H and ^{13}C resonances were fully assigned by 1D and 2D (^{1}H-^{1}H correlation spectroscopy [COSY], ^{1}H-^{1}H total COSY [TOCSY], and ^{1}H-^{13}C heteronuclear single quantum coherence spectroscopy [HSQC]) NMR experiments (see *Supporting Information*). The sites of sulfation were confirmed by downfield shifts of ring protons (≈0.5 ppm) and by downfield shift of ring carbons (≈4 ppm). Furthermore, complete *O*- and *N*-sulfation results in appearance of peaks corresponding to C-2$_{GlcN}$, C-6$_{GlcN}$ and C-2$_{IdoA}$ as distinct clusters (see HSQC NMR spectra in *Supporting Information*).

Evaluation of HS oligosaccharides as Hpse inhibitors

HS oligosaccharides **1**–**6** bear only IdoA moieties in their backbones and therefore it was expected that they will be resistant to hydrolysis by Hpse. To biochemically confirm this resistance, we employed a colorimetric assay based on detection of newly formed reducing ends upon cleavage of scissile bonds by Hpse employing the water soluble tetrazole reagent-1 (WST-1, Figure 2A).[15] Thus, compound **1**–**6** (50 μM) and Fondaparinux (Fpx., positive control) were incubated at 37 °C with Hpse (50 nM) and reactions were developed by treatment with WST-1 (at 60 °C for 1 h). Notably, none of the oligosaccharides were cleaved by Hpse even after an incubation time of 16 h (Figure 2B).

The inhibitory potential of the synthetic compounds was evaluated by a homogeneous time-resolved fluorescence assay (HTRF®, CisBio/PerkinElmer).[16] This assay is based on Förster resonance energy transfer (FRET) between two fluorophores; a donor (europium cryptate, K) and an acceptor (allophycocyanin, XL665). The time-resolved (TR) component eliminates short-lived background fluorescence

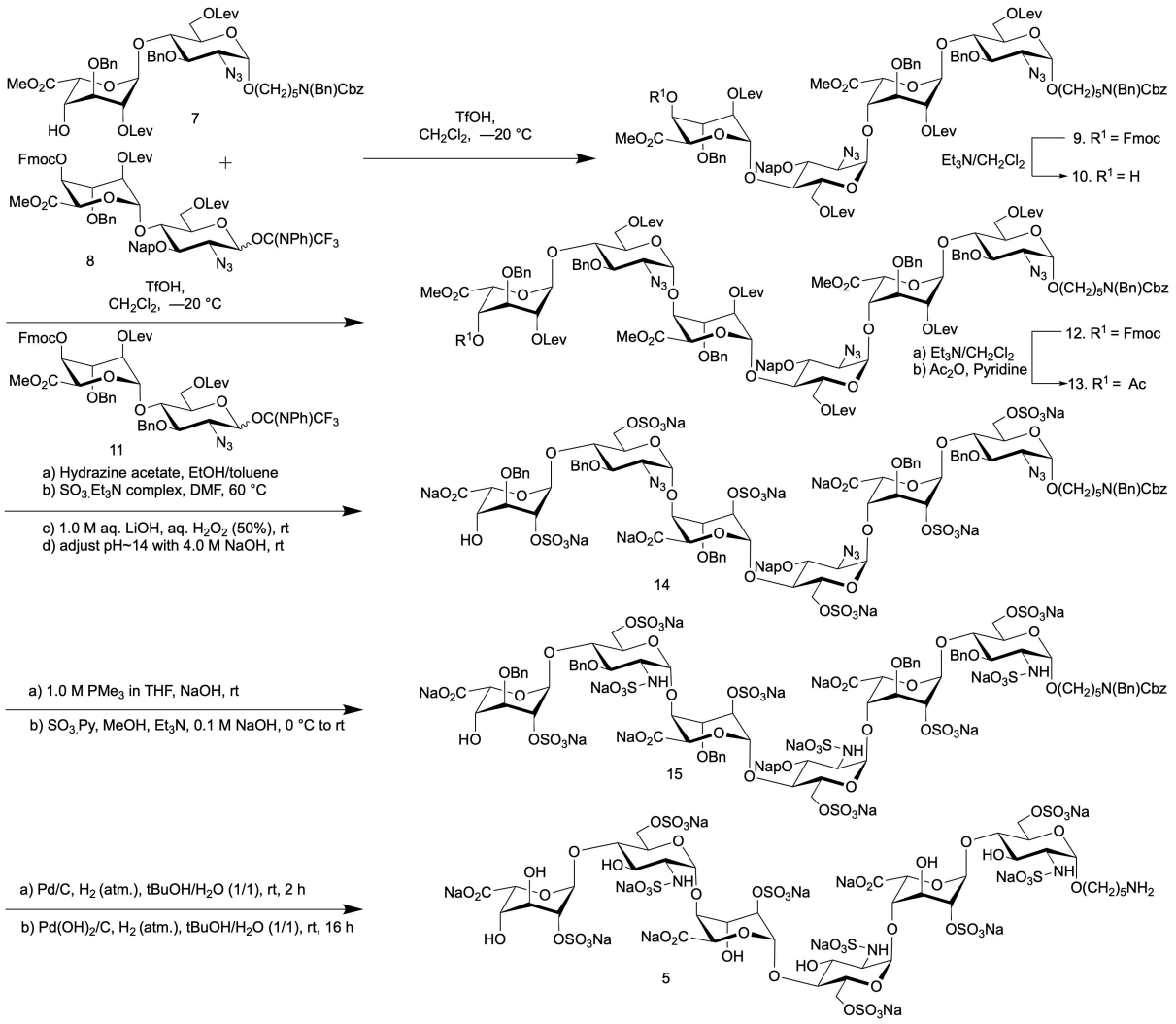

Scheme 1. Modular synthesis of hexasaccharide **5**.

which in combination with large Stokes shift makes the assays highly sensitive.[24] The HTRF® heparanase assay utilizes a bifunctional HS substrate (biotin-HS-K) labeled with europium cryptate and biotin. The biotin moiety of the HS substrate interacts with streptavidin-XL665 to form a FRET donor-acceptor complex which upon cleavage by Hpse is lost (Figure 2C). First, we incubated biotin-HS-K either with Hpse or buffer control at 37 °C for 1 h, followed by the addition of XL665 at room temperature for 20 min. As anticipated, in the presence of Hpse the substrate was hydrolysed and no FRET signal was observed, whereas the control reaction, in which the substrate is still intact, gave a strong signal (Figure S2). Next, a wide range of concentrations of compounds **1**–**6** were employed in the HTRF® assay and half-maximal inhibitory concentrations (IC_{50} values) were determined by nonlinear regression of log(inhibitor) vs. response-variable slope (Figure 2D and Figure S3). It was found that compounds having a 2-OS moiety were somewhat more potent inhibitors than the corresponding oligosaccharides lacking this moiety (**1** vs. **2** and **3** *vs.* **4**). Furthermore, by increasing the chain length, the inhibitory potential increased substantially (**1** vs. **3** vs. **5** vs. **6**), and compound **6** exhibited an IC_{50} value of 1.1 μM (Figure 2F). To examine whether a further increase in HS oligosaccharide chain length will result in subsequent improvement in inhibitory activity, isolated heparin oligomers (Iduron, UK) with degree of polymerization (DP) of 10, 12 and 14 were investigated (Figure S4A). The DP-12 and −14 oligomers gave IC_{50} value of 0.38 and 0.14 μM, respectively (Figure S4B–D), indicating that by using longer HS oligomers the activity can be further improved.

Enzyme kinetic studies can provide further insight in mode of inhibition of the synthetic compounds. To reliably characterize inhibition kinetics, full length HS is an unsuitable substrate because it is heterogeneous and provide multiple points of cleavage. Furthermore, fragments produced by the action of Hpse may invoke inhibition. In contrast, the pentasaccharide Fpx., which is clinically employed as an anti-coagulating agent, has a GlcA moiety that can be cleaved by Hpse introducing a reducing end that can be detected by WST-1.[15] Therefore, oligosaccharides **1**–

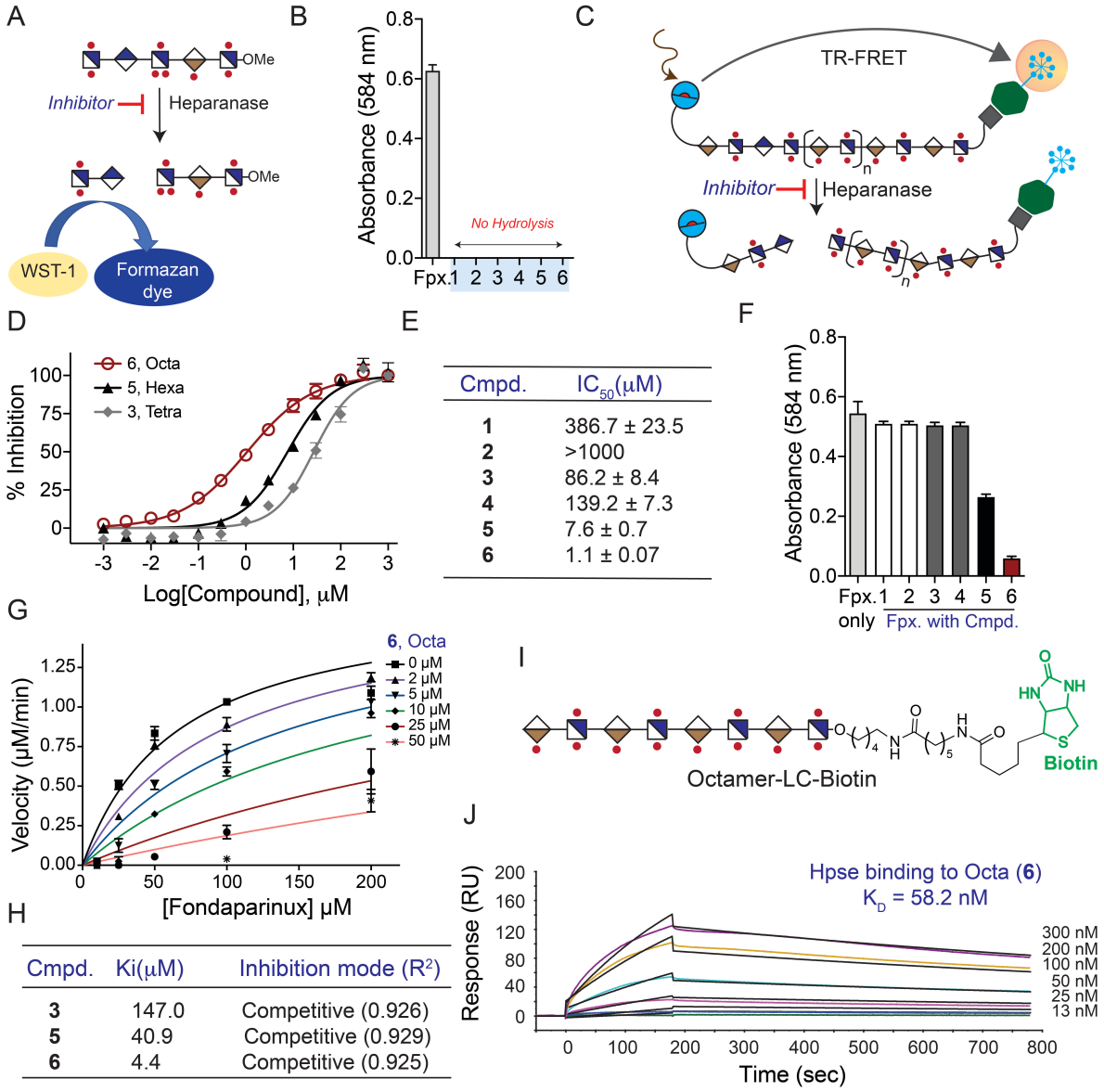

Figure 2. Biochemical and biophysical evaluation of compound **1**–**6**. (A) Schematic diagram for WST-1 assay; (B) Hydrolysis assays; (C) Schematic diagram for TR-FRET assay; (D) IC_{50} determination using TR-FRET assays; (E) Summary table of IC_{50}; (F) Inhibitor screening using WST-1 assay; (G) Kinetic measurements to determine the inhibition constant (*Ki*) value of compound **6** (4.4 μM); (H) Summary table of *Ki* value, inhibition mode and coefficient of determination (R^2); (I) Structure of biotinylated octamer (**16**); (J) Surface plasmon resonance (SPR) sensorgram of Hpse binding with **16**. Data are presented as mean ± SD ($n = 3$), representative experiments are shown which have been repeated at least three times.

6 were examined as inhibitors of Hpse mediated hydrolysis of Fpx. at an initial concentration of 50 μM (Figure 2F).

Hexasaccharide **5** and octasaccharide **6** showed promising inhibitory activities, while disaccharides **1** and **2** and tetrasaccharides **3** and **4** showed no detectable activity at the screening concentration. Next, inhibitory constants (K_i) of compounds **5** and **6** were determined by incubating various concentration of Fpx. (10 μM to 200 μM) with Hpse in the presence of inhibitors (**5** or **6**, 2 to 50 μM) and fitting the data to enzyme kinetics-inhibition equations built in Prism software. Good fits for competitive inhibition were obtained giving a *Ki* of 40.9 μM ($R^2 = 0.929$) for **5** and 4.4 μM ($R^2 = 0.929$) for **6** (Figure 2G–H and Figure S1).

Next, the binding affinity of the most potent inhibitor (**6**) for Hpse was evaluated by surface plasmon resonance (SPR). Thus, compounds **6** was biotinylated by coupling the anomeric aminopentyl linker with sulfo-*N*-hydroxysuccinamide-long chain (LC)-biotin to afford Octamer-LC-biotin (**16**, Figure 2I), which was immobilized on the streptavidin-functionalized CM5 sensor chip. Binding experiments were performed by employing different concentrations of the Hpse as analytes (Figure 2J, representative sensorgram of three independent runs is presented) and equilibrium dissociation constant (K_D) value of 58 nM was determined using a 1:1 Langmuir binding model (For detailed fitting data see Figure S5).

Molecular modelling to rationalize inhibition data

To rationalise the observed differences in inhibition potency, we performed docking studies of compounds **1**, **3**, **5**, and **6** with Hpse.[25] The 3D structures of the oligosaccharides were built using the GLYCAM carbohydrate builder web tool (http://glycam.org) and energy minimized by GROMACS.[26] The resulting structures were superimposed to the tetrasaccharide ΔDP-4: ΔHexUA2S-GlcNS6S-IdoA-GlcNS6S observed in a co-crystal with Hpse (PDB: 5E9C)[18] using the PyMol alignment tool.[27] In particular, the first internal IdoA2S residue from the non-reducing end, was superimposed onto the IdoA ring of the ΔDP-4 which occupies the catalytic site of the enzyme (−1 site). After ligand replacement, the resulting structures were energy minimized and analysed for intermolecular interactions. It showed that the oligosaccharides can establish several intermolecular interactions with Hpse in a size-dependent manner. We observed engagement of the positively charged amino acids within the cleft of Hpse by sulfates of the oligosaccharides leading to shape complementarity. Octasaccharide **6** established 26 intermolecular interactions, of which 14 are hydrogen bonds and 12 are electrostatic (Figure 3A–C and Table S1). Similarly, the hexasaccharide **5** established 24 polar intermolecular interactions, 13 of which are hydrogen bonds and 11 are electrostatic (Figure S9 and Table S2). The tetrasaccharide **3** established 21 intermolecular interactions of which 11 are hydrogen bonds and 10 are electrostatic (Figure S10 and Table S3), while the disaccharide **1** made 16 interactions of which 11 are hydrogen bonds and only five are electrostatic (Figure S11 and Table S4). The difference in the number of intermolecular interactions correlates with their IC_{50} values. While the intermolecular interactions at the catalytic sites −1 and +1 are preserved for all studied oligosaccharides, the main difference lies in the contribution of the residues upstream and downstream of the cleft and in the case of larger hexa- and octasaccharides additional contacts could be made whereas this is not the case for the di- and tetrasaccharide.

To investigate how the enzyme accommodates IdoA2S at the catalytic site −1, the 3D structure of IdoA2S-GlcNS6S-OMe was built and superimposed on the ΔDP-4 bound to Hpse (PDB: 5E9C). As expected, the presence of the sulfate group at the C-2 of the IdoA generated steric clashes with some residues within the catalytic pocket (Glu343, His296, and Asn224). After energy minimization, the resulting structure showed a rearrangement of several side chains of the residues surrounding the sulfate group (Figure 3D–E and Figure S6). As result, a larger cavity was formed to host the sulfate. In this cavity, Thr97, Asn224,

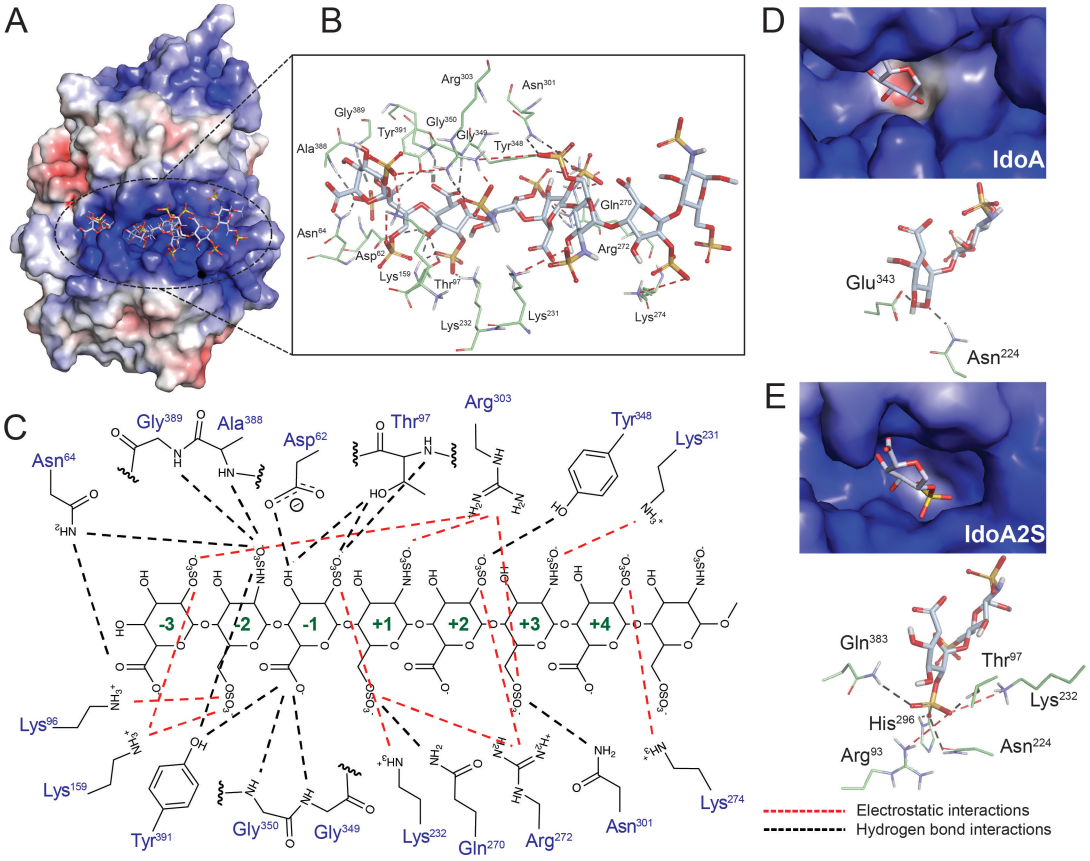

Figure 3. Docked structure of the Hpse in complex with **6**. (A) Surface and stick representation, electrostatic potential surface, coloured by charge density; (B) Stick representation of the protein residues interacting with **6**; (C) Schematic representation of the intermolecular interactions, electrostatic interactions; (D) Differences in IdoA and (E) IdoA2S binding at the Hpse catalytic site.

His296, and Gln383 established hydrogen bonds with the sulfate, while residues Arg93 and Lys232 participated by electrostatic interactions through their positively charged side chains (Figure 3E).

A comparison with the above-mentioned crystal structure of Hpse showed that the hydroxyl group at C-2 of IdoA forms hydrogen bonds with Asn224 and Glu343 (Figure 3D). Glu343 has been identified as one of the two nucleophilic catalytic residues together with Glu225. Interestingly, the replacement of the hydroxyl by a sulfate moves back the negatively charged side chain of the Glu343 due to the repulsive electrostatic interaction. The larger distance between the carboxylate of the Glu343 and the anomeric carbon of the IdoA ring of the substrate may contribute to the resistance of IdoA2S-containing oligosaccharides to Hpse-mediated hydrolysis.

Hpse inhibitors block viral egress by inhibiting shedding of cell surface HS during HSV-1 infection

Previously, we described that in response to HSV-1 infection, the expression of Hpse is upregulated, which results in HS shedding allowing outgoing virions to escape and spread to other cells.[14,28] We hypothesized that inhibition of Hpse by compounds **5** and **6** will prevent virus induced HS degradation which in turn should block viral release. Thus, we pre-treated (−2 hours post-infection, hpi), neutralized (0 hpi) or therapeutically (2–12 hpi) administered compounds **5** or **6** to HCEs[29] infected with HSV-1 strain 17GFP, and examined the plaque count of viruses that remained associated with cells or released into the media.[30] The administration of compounds **5** and **6** at different time points during the infection experiments allowed for the identification of specific stages in the viral life cycle that are affected. The introduction of the compounds after infection, particularly at late time points (8 and 12 hpi), is expected to primarily influence viral release. On the other hand, pretreatment of the cells (−2 hpi) or simultaneous administration of the compound (0 hpi) along with the virus have a more significant impact on viral attachment and entry. At 24 hpi, cell lysates containing intracellular virus and supernatants containing extracellular egressed virus were collected and overlaid on Vero cells to perform plaque assays to count infectious particles (Figure 4A–B). As expected, there were substantial reductions in extracellular virus in the samples that were treated pre- or post-infection with **5** and **6**. Importantly, a large reduction was observed even when the inhibitors were administrated at 8 or 12 hpi supporting the notion the HS-oligosaccharides suppress viral release. To quantify the potency of the compounds in restricting viral spread, a fluorescence-based inhibition assays was performed using green fluorescent protein (GFP)-reporter virus at low multiplicity of infection (MOI, number of virions added per cell).[31] In this assay, viral spread can be quantified between control groups by measuring the percentage of GFP positive cells. Thus, HCEs were infected with 17 GFP virus at 0.1 MOI and at 2 hpi different concentrations of compounds **5**, **6**, and UFH were added. After 24 h, the ratio of infected cells (GFP-positive) vs. total cells (DAPI nuclear stain) was assessed to determine IC_{50} values (Figure S12). In the absence of HS oligosaccharides or heparin, all cells were GFP positive demonstrating that viral spread had occurred. Both **5** and **6** inhibited HSV-1 spread and gave an IC_{50} value of 55 μg/mL and 42 μg/mL, respectively. Unfractionated heparin (UFH) is more potent inhibitor with an IC_{50} value of 1 μg/mL.

To evaluate possible inhibition of viral attachment and entry into HCEs by compounds **5**, **6** and UFH, a recombinant virus (KOS gL86) was employed,[32] which expresses β-galactosidase derived from the lacZ gene that has been substituted for the gL gene that encodes a fusion glycoprotein. HCEs were concurrently exposed to the KOS gL86 virus and compound **5**, **6** and UFH. The infection was allowed to continue for 6 h, facilitating β-galactosidase production, thereby serving as an indicator of viral entry. The levels of β-galactosidase activity were quantified using ortho-nitrophenyl β-D-galactopyranoside (ONPG) as a substrate. It was observed that all compounds robustly inhibited β-galactosidase activity, indicating that they also act as entry inhibitors. UFH impeded HSV-1 entry into HCEs with an IC_{50} value of 2 μg/mL, while compounds **5** and **6** displayed IC_{50} values of 27 μg/mL and 22 μg/mL, respectively (Figure S13). Collectively, these results indicate that compounds **5** and **6** have a dual mode of action and can inhibit viral entry as well as release.

We performed additional studies to confirm that the reduction in egressed virus is due to blocking of virus-induced cell surface HS shedding. Thus, 2 h after mock or infection with HSV-1, HCEs were treated with compounds **5** or **6**, and HS expression was examined 24 h post-infection by fluorescence microscopy using an anti-HS antibody (10E4 epitope)[14] and a secondary antibody labeled with Alexa-Fluor-546. Cells were stained with the antibodies prior to fixation to ensure only cell surface HS was detected (Figure 4D). As expected, HSV-1 infection of HCEs resulted in the significant loss of cell surface HS. However, mean intensity density analysis of fluorescence intensities of HCEs treated with **5** and **6** showed substantially higher levels of cell surface HS, which was like that of non-infected cells (Figure 4E).

These results indicate that compounds **5** and **6** prevent removal of HS from the cell surface during HSV-1 infection. Additional flow cytometry analysis was performed to quantify and compare cell surface HS expression more accurately. As can been seen in Figure 4E–F, the number of cells that were positive for cell surface HS was much greater in samples treated with **5** and **6** during HSV-1 infection, further confirming that inhibition of Hpse prevents virus induced HS-shedding. It is of interest to note that there was no difference in non-infected samples that were treated with **5** or **6** indicating that the compounds do not interfere with baseline surface HS turnover.

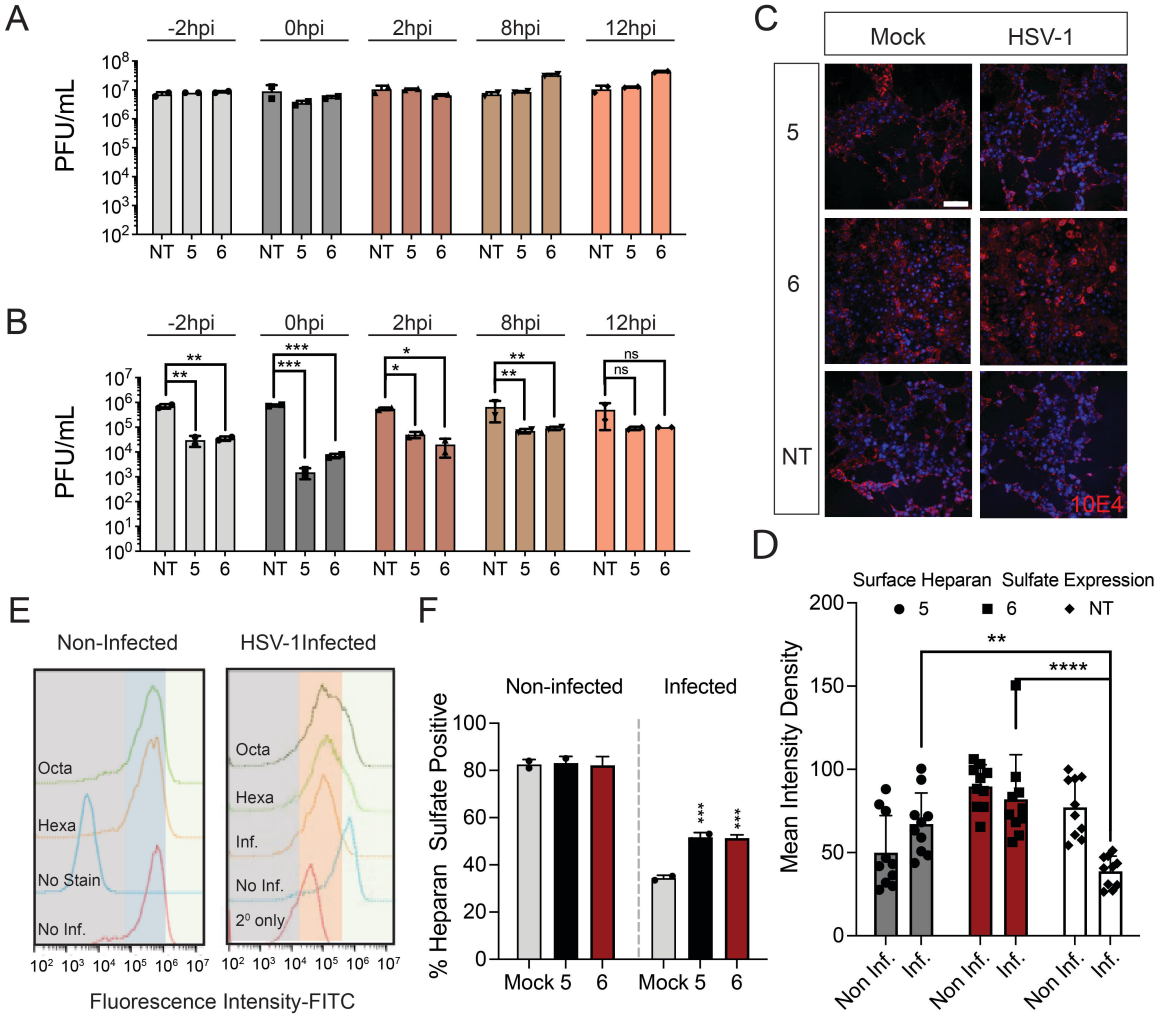

Figure 4. HPSE inhibitors **5** and **6** decrease viral egress from HSV-1 infected HCEs. (A) Plaque assay analysis comparing extracellular and intracellular virus; (B) Extracellular virus collected from the cell supernatants for all time points were titrated and plaque counts are shown; (C) Addition of **5** and **6** sequesters cell surface HS during HSV-1 infection; (D) Quantification of Figure 4C; (E) Flow cytometry evaluation of HS shedding in infected HCEs; (F) Quantification of flow cytometry analysis conducted in Figure 4E. Data are presented as mean ± SEM ($n = 3$), representative experiments are shown which have been repeated at least three times.

Inhibition of cell migration and proliferation

In addition to being a pro-viral and pro-inflammatory factor, Hpse activity has been linked to various pro-survival activities such as cell migration, and proliferation.[33] It has been shown that exogenous administration of Hpse stimulates phosphatidylinositol 3-kinase (PI3 K)-dependent endothelial cell migration and proliferation.[34] On the other hand, inhibition of Hpse suppresses cell migration and proliferation of non-infected cells.[35] Previously, we have shown that HSV-1 infected murine corneas that overexpress a constitutively active form of Hpse in the epithelium have reduced wound healing capacity.[36] We hypothesized that compounds **5** and **6** will improve HCEs wound healing ability by suppressing viral-induced Hpse activity.

Monolayer scratch assays are a cost effective and time efficient approach to determine the migratory potential of the cells in vitro.[37] Therefore, confluent monolayers of HCEs were disjointed by a single ≈100 μm scratch followed by infection with mock or HSV-1 and the addition of **5**, **6** or vehicle control. Cells from the edge of the scratch would migrate to the center and inhibition of Hpse was expected to slow this activity. The migration site was monitored for a period of 24 h by taking images at hourly intervals (Figure 5A, non-infected and Figure 5C, HSV-1 infected). The migration assay images were analyzed and the % of uncovered area was calculated in each frame of the image (Figure 5B and 5D). Compounds **5** and **6** caused a significant decrease in migration only allowing ≈75 % and 50 % coverage of the migration site, respectively in non-infected HCEs.

Previously, we demonstrated that the expression and activity of Hpse increases upon HSV-1 infection.[36] The elevated Hpse activity corresponds with accelerated cell migration, which is also evident from the results presented here. However, starting at 12 hpi, the cells start to circularize and undergo cell death leading to an increase in uncovered

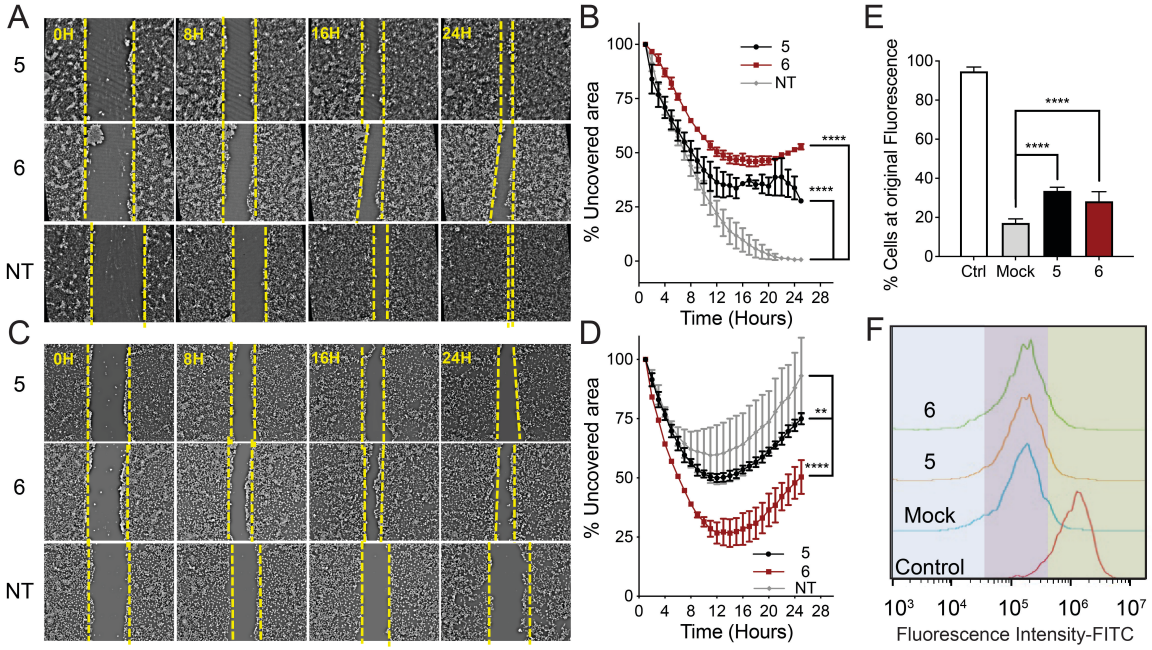

Figure 5. Cell migration and cell proliferation is restricted by **5** and **6**. (A) Image of the scratch site to monitor extent of migration of cells; (B) Quantification of uncovered area from Figure 5A; (C) Image of the scratch site to monitor HSV-1 infected cells; (D) Quantification of % uncovered area for images taken in Figure 5C; (E) Cell proliferation assays via flow cytometry; (F) Quantification of Figure 5E. Data are presented as mean ± SEM ($n = 3$), representative experiments are shown which have been repeated at least three times.

area. As illustrated in Figure 5B, the non-treated cells showed diminished wound healing capabilities primarily due to extensive infection and cell death. On the other hand, cells treated with **5** and **6** exhibited a significant increase in migration, indicating improved wound healing abilities that can be attributed to the antiviral activity of **5** and **6**, as described above.

To examine whether the addition of Hpse inhibitors such as **5** and **6** cause a decrease in cell proliferation, we monitored cell proliferation of HCEs using CytoPainter assay. This assay is similar to a traditional Carboxyfluorescein succinimidyl ester (CFSE) assay where cells are initially dyed with the CFSE dye, and the mean fluorescence intensity depletes during every cell division cycle.[38] We performed a flow cytometric analysis of cells treated with **5** and **6** to determine the extent of cells retaining original fluorescence intensity (Figure 5E–F). Quantitative analysis of the flow cytometry showed that **5** and **6** treated populations had significantly higher cells retaining the original fluorescence intensity when compared to vehicle control treated population. These results indicate that **5** and **6** inhibit cell-migration and proliferation in HCEs.

Evaluation of anticoagulation and cytotoxic effects

The use of heparin as a therapeutic is complicated by structural heterogeneity and the risk of causing bleeding and thrombocytopenia.[39] The hexa- and octa-saccharide described here are devoid of 3-*O*-sulfated GlcNS which is critical for the anticoagulation activity of heparin. To confirm this lack of activity, we measured AT-III mediated anti-Factor-IIa and anti-Factor-Xa activities of compounds **5**, **6**, and UFH using a colorimetric assay (Biophen Anti-IIa and Anti-Xa kits, two-stage chromogenic assays) (Figures S15–S17). As anticipated, UFH gave an IC_{50} value of 0.1 μg/mL for Factor-IIa (Figure S16) and 0.1 μg/mL for Factor-Xa (Figure S17). Compounds **5** and **6** did not show any inhibition of Factor-IIa and inhibited Factor-Xa with high IC_{50} values of 85 and 52 μg/mL, respectively (Figures S16 and S17).

The cytotoxicity of compounds **5**, **6**, and UFH was evaluated on HCE cells using the 3-(4,5-dimethylthiazol-2-yl)-2,5-diphenyltetrazolium bromide (MTT) colorimetric assay. It was found that compound **5** (8–1000 μM, 24 h), **6** (8–1000 μM, 24 h), and UFH **5** (0.8–100 μg/mL, 24 h) did not affect the viability of HCEs and exhibits no toxicity (Figure S14).

Conclusion

We have designed and prepared a range of HS oligosaccharides to examine the importance of chain length and 2-*O*-sulfation of IdoA for Hpse inhibitory activity. In two different assay formats it was found that by increasing the chain length of IdoA containing oligosaccharides the inhibitory activity substantially improved. An octasaccharide composed of IdoA2S-GlcNS6S repeating units competitively inhibited the cleavage of Fpx. with *Ki* of 4.4 μM. Docking studies showed that the binding cleft of Hpse can accomodate an octasaccharide and that each monosaccharide

residue can establish electrostatic interactions and/or hydrogen bonds with the protein. The inhibition studies also showed that HS oligosaccharides having 2-*O*-sulfate moieties can be accommodated by Hpse. The computational studies indicated that in this binding mode catalytic residues at the −1 subsite are displaced, which may contribute to resistance to hydrolysis. It is known that heparin, which is rich in IdoA2S-GlcNS6S moieties, can inhibit Hpse.[4–6] The studies presented here support that IdoA2S-containing residues within heparin contribute to its inhibitory activity. HS has much lower levels of sulfation, and structural motifs such as that of hexasaccharide **5** and octasaccharide **6** are very rare in HS. Thus, cell surface HS may have a much lower propensity to inhibit Hpse than heparin. The use of heparin as a therapeutic is complicated by structural heterogeneity and the risk of causing bleeding and thrombocytopenia. The hexa- and octasaccharides described here are devoid of 3-*O*-sulfated GlcNS which is critical for the anticoagulation activity of heparin and, as expected, did have no or very reduced activity for Factor-IIa and Factor-Xa, respectively.

Previous studies have shown that the modification of sulfated oligosaccharides with a lipophilic aglycon can improve Hpse inhibitors potency.[40] Multivalent display of sulfated oligosaccharides is another approach to improve the inhibitory activity of sulfated oligosaccharide.[41] Also, HS-configured cyclophellitol pseudo-disaccharides have been reported to be highly active mechanism-based Hpse inhibitors.[42] A future goal is to examine if the inhibitory potential of compounds such as **5** and **6** can be improved by such approaches.

HSV-1 employs HS as receptor for cell attachment and entry. Previously, we showed that during late-stage infection, the virus induces the upregulation of Hpse to remove cell surface HS allowing detachment of newly formed virions from cells.[7,13b] We also showed that genetic knockdown of Hpse in vivo results in significant reduction of viral shedding. Therefore, we anticipated that pharmacological inhibition of Hpse by compounds such as **5** and **6** may also prevent viral release thereby exerting a therapeutic effect. To test this hypothesis, detailed kinetic infection studies were performed in which compounds **5** and **6** were administered pre- or post HSV-1 challenge followed by examination of the number of virions associated with cells and released into the media. Treatment of HSV-1 infected cells as late as 8 and 12 hpi with the HS oligosaccharides resulted in a very significant reduction in released virions. Moreover, the HS-oligosaccharide prevented HSV-1 induced shedding of cell surface HS from immortalized HCE cells. Combined, these observations support the notion that inhibition of Hpse by compounds such as **5** and **6** can reduce viral release and spread.

It is possible that administration of the HS oligosaccharides before or at the same time of HSV-1 challenge may also inhibit cell attachment and entry. Therefore, viral entry studies were performed using the recombinant virus, KOS gL86, in which the gene for a fusion glycoprotein (gL) is replaced by the lacZ gene that encodes a β-galactosidase.[43] It was found that the HS oligosaccharides inhibit β-galactosidase activity indicating that they have a dual mode of action by impeding viral entry as well as release. The greatest reduction in released virus was observed when the compounds were administered pre- or at the time of infection (Figure 4B), which agrees with a dual mode of action.

The biological activity of the HS oligosaccharides was further demonstrated by their ability to inhibit the migration and proliferation of HCEs. Hpse plays an important role in the progression of ocular herpes pathogenesis by promoting the formation of new blood vessels (angiogenesis), which allow immune cells to migrate into the corneal tissue causing corneal opacity and inflammation resulting in herpes keratitis, a major contributor to infectious blindness. Inhibition of Hpse in corneal cells is important for wound healing and modulation of ocular inflammation. Collectively, these observations demonstrate that Hpse inhibitors can prevent viral release and subsequent spread to other cells and tissues.

Supporting Information

Supporting Information for this article is available with detailed synthetic protocols, compound characterization, enzyme inhibition assays, SPR data, molecular modelling, virology data, and NMR spectra (PDF).

Acknowledgements

This research was supported by the National Institutes of Health (P41GM103390 and HLBI R01HL151617 to G.-J.B.; R01EY029426, R01EY024710, and P30EY001792 to D.S.). We thank Dr. Apoorva Joshi and Dr. Vito Thijssen for technical assistance. We thank Dr. Gideon J. Davies (University of York, York, UK) for providing human heparanase.

Conflict of Interest

The authors declare no conflict of interest.

Data Availability Statement

The data that support the findings of this study are available in the supplementary material of this article.

Keywords: Antivirals · Drug Discovery · Heparanase · Heparin · Herpes Simplex Virus Type 1

[1] a) C. R. Parish, C. Freeman, M. D. Hulett, *Biochim. Biophys. Acta Rev. Cancer* **2001**, *1471*, M99-M108; b) I. Vlodavsky, Y. Friedmann, *J. Clin. Invest.* **2001**, *108*, 341–347.

[2] S. Sarrazin, W. C. Lamanna, J. D. Esko, *Cold Spring Harbor Perspect. Biol.* **2011**, *3*, a004952.

[3] a) D. S. Pikas, J.-P. Li, I. Vlodavsky, U. Lindahl, *J. Biol. Chem.* **1998**, *273*, 18770–18777; b) Y. Okada, S. Yamada, M. Toyoshima, J. Dong, M. Nakajima, K. Sugahara, *J. Biol. Chem.* **2002**, *277*, 42488–42495; c) S. B. Peterson, J. Liu, *J. Biol. Chem.* **2010**, *285*, 14504–14513.

[4] S. Rivara, F. M. Milazzo, G. Giannini, *Future Med. Chem.* **2016**, *8*, 647–680.

[5] I. Vlodavsky, N. Ilan, R. D. Sanderson, *Adv. Exp. Med. Biol.* **2020**, *1221*, 3–59.

[6] a) E. A. McKenzie, *Br. J. Pharmacol.* **2007**, *151*, 1–14; b) C. D. Mohan, S. Hari, H. D. Preetham, S. Rangappa, U. Barash, N. Ilan, S. C. Nayak, V. K. Gupta, Basappa, I. Vlodavsky, K. S. Rangappa, *iScience* **2019**, *15*, 360–390; c) D. R. Coombe, N. S. Gandhi, *Front. Oncol.* **2019**, *9*, 1316.

[7] N. Thakkar, T. Yadavalli, D. Jaishankar, D. Shukla, *Pathogenesis* **2017**, *6*, 43.

[8] R. J. Whitley, B. Roizman, *Lancet* **2001**, *357*, 1513–1518.

[9] L. Koujah, R. K. Suryawanshi, D. Shukla, *Cell. Mol. Life Sci.* **2019**, *76*, 405–419.

[10] M. K. Kukhanova, A. N. Korovina, S. N. Kochetkov, *Biochemistry* **2014**, *79*, 1635–1652.

[11] D. Shukla, P. G. Spear, *J. Clin. Invest.* **2001**, *108*, 503–510.

[12] a) P. G. Spear, R. J. Eisenberg, G. H. Cohen, *Virology* **2000**, *275*, 1–8; b) P. G. Spear, *Cell. Microbiol.* **2004**, *6*, 401–410.

[13] a) V. Tiwari, M. S. Tarbutton, D. Shukla, *Molecules* **2015**, *20*, 2707–2727; b) A. Banerjee, S. Kulkarni, A. Mukherjee, *Front. Microbiol.* **2020**, *11*, 733.

[14] S. R. Hadigal, A. M. Agelidis, G. A. Karasneh, T. E. Antoine, A. M. Yakoub, V. C. Ramani, A. R. Djalilian, R. D. Sanderson, D. Shukla, *Nat. Commun.* **2015**, *6*, 6985.

[15] E. Hammond, C. P. Li, V. Ferro, *Anal. Biochem.* **2010**, *396*, 112–116.

[16] S. Roy, A. El Hadri, S. Richard, F. Denis, K. Holte, J. Duffner, F. Yu, Z. Galcheva-Gargova, I. Capila, B. Schultes, M. Petitou, G. V. Kaundinya, *J. Med. Chem.* **2014**, *57*, 4511–4520.

[17] J. C. Wilson, A. E. Laloo, S. Singh, V. Ferro, *Biochem. Biophys. Res. Commun.* **2014**, *443*, 185–188.

[18] L. Wu, C. M. Viola, A. M. Brzozowski, G. J. Davies, *Nat. Struct. Mol. Biol.* **2015**, *22*, 1016–1022.

[19] S. Zhu, J. Li, R. S. Loka, Z. Song, I. Vlodavsky, K. Zhang, H. M. Nguyen, *J. Med. Chem.* **2020**, *63*, 4227–4255.

[20] A. Naggi, B. Casu, M. Perez, G. Torri, G. Cassinelli, S. Penco, C. Pisano, G. Giannini, R. Ishai-Michaeli, I. Vlodavsky, *J. Biol. Chem.* **2005**, *280*, 12103–12113.

[21] A. Alekseeva, B. Casu, G. Cassinelli, M. Guerrini, G. Torri, A. Naggi, *Anal. Bioanal. Chem.* **2014**, *406*, 249–265.

[22] S. Arungundram, K. Al-Mafraji, J. Asong, F. E. Leach, I. J. Amster, A. Venot, J. E. Turnbull, G.-J. Boons, *J. Am. Chem. Soc.* **2009**, *131*, 17394–17405.

[23] P. Chopra, A. Joshi, J. Wu, W. Lu, T. Yadavalli, M. A. Wolfert, D. Shukla, J. Zaia, G.-J. Boons, *Proc. Natl. Acad. Sci. USA* **2021**, *118*, e2012935118.

[24] A. R. Holzwarth, *Methods in Enzymology, Vol. 246*, Academic Press, New York, **1995**, pp. 334–362.

[25] a) G. M. Morris, R. Huey, W. Lindstrom, M. F. Sanner, R. K. Belew, D. S. Goodsell, A. J. Olson, *J. Comput. Chem.* **2009**, *30*, 2785–2791; b) O. Trott, A. J. Olson, *J. Comput. Chem.* **2010**, *31*, 455–461; c) A. K. Nivedha, D. F. Thieker, H. Hu, R. J. Woods, *J. Chem. Theory Comput.* **2016**, *12*, 892–901.

[26] M. J. Abraham, T. Murtola, R. Schulz, S. Páll, J. C. Smith, B. Hess, E. Lindahl, *SoftwareX* **2015**, *1–2*, 19–25.

[27] L. Schrödinger, W. DeLano, http://www.pymol.org/pymol, **2020**.

[28] J. Hopkins, T. Yadavalli, A. M. Agelidis, D. Shukla, *J. Virol.* **2018**, *92*, e01179–01118.

[29] A. Shah, A. V. Farooq, V. Tiwari, M. J. Kim, D. Shukla, *Mol. Vision* **2010**, *16*, 2476–2486.

[30] a) T. Yadavalli, J. Ames, A. Agelidis, R. Suryawanshi, D. Jaishankar, J. Hopkins, N. Thakkar, L. Koujah, D. Shukla, *Sci. Adv.* **2019**, *5*, eaax0780; b) T. Yadavalli, R. Suryawanshi, M. Ali, A. Iqbal, R. Koganti, J. Ames, V. K. Aakalu, D. Shukla, *Ocul. Surf.* **2020**, *18*, 221–230.

[31] C. E. Lilley, C. T. Carson, A. R. Muotri, F. H. Gage, M. D. Weitzman, *Proc. Natl. Acad. Sci. USA* **2005**, *102*, 5844–5849.

[32] R. I. Montgomery, M. S. Warner, B. J. Lum, P. G. Spear, *Cell* **1996**, *87*, 427–436.

[33] a) N. Ilan, M. Elkin, I. Vlodavsky, *Int. J. Biochem. Cell Biol.* **2006**, *38*, 2018–2039; b) I. Vlodavsky, O. Goldshmidt, E. Zcharia, R. Atzmon, Z. Rangini-Guatta, M. Elkin, T. Peretz, Y. Friedmann, *Semin. Cancer Biol.* **2002**, *12*, 121–129.

[34] a) A. Riaz, N. Ilan, I. Vlodavsky, J.-P. Li, S. Johansson, *J. Biol. Chem.* **2013**, *288*, 12366–12375; b) G. Che, Y. Wang, B. Zhou, L. Gao, T. Wang, F. Yuan, L. Zhang, *Dis. Markers* **2018**, *2018*, 7413027.

[35] a) O. Lider, Y. A. Mekori, T. Miller, R. Bar-Tana, I. Vlodavsky, E. Baharav, I. R. Cohen, Y. Naparstek, *Eur. J. Immunol.* **1990**, *20*, 493–499; b) S. M. Courtney, P. A. Hay, R. T. Buck, C. S. Colville, D. J. Phillips, D. I. C. Scopes, F. C. Pollard, M. J. Page, J. M. Bennett, M. L. Hircock, E. A. McKenzie, M. Bhaman, R. Felix, C. R. Stubberfield, P. R. Turner, *Bioorg. Med. Chem. Lett.* **2005**, *15*, 2295–2299.

[36] A. M. Agelidis, S. R. Hadigal, D. Jaishankar, D. Shukla, *Cell Rep.* **2017**, *20*, 439–450.

[37] Y. Zhang, G. S. Chia, C. Y. Tham, S. Jha, *J. Visualized Exp.* **2017**, *130*, e56248.

[38] B. J. Quah, C. R. Parish, *J. Visualized Exp.* **2010**, *44*, e2259.

[39] A. Onishi, K. S. Ange, J. S. Dordick, R. J. Linhardt, *Front. Biosci.* **2016**, *21*, 1372–1392.

[40] V. Ferro, L. Liu, K. D. Johnstone, N. Wimmer, T. Karoli, P. Handley, J. Rowley, K. Dredge, C. P. Li, E. Hammond, K. Davis, L. Sarimaa, J. Harenberg, I. Bytheway, *J. Med. Chem.* **2012**, *55*, 3804–3813.

[41] a) R. S. Loka, F. Yu, E. T. Sletten, H. M. Nguyen, *Chem. Commun.* **2017**, *53*, 9163–9166; b) O. V. Zubkova, Y. A. Ahmed, S. E. Guimond, S.-L. Noble, J. H. Miller, R. A. Alfred Smith, V. Nurcombe, P. C. Tyler, M. Weissmann, I. Vlodavsky, J. E. Turnbull, *ACS Chem. Biol.* **2018**, *13*, 3236–3242.

[42] C. de Boer, Z. Armstrong, V. A. J. Lit, U. Barash, G. Ruijgrok, I. Boyango, M. M. Weitzenberg, S. P. Schröder, A. J. C. Sarris, N. J. Meeuwenoord, P. Bule, Y. Kayal, N. Ilan, J. D. C. Codée, I. Vlodavsky, H. S. Overkleeft, G. J. Davies, L. Wu, *Proc. Natl. Acad. Sci. USA* **2022**, *119*, e2203167119.

[43] D. Shukla, J. Liu, P. Blaiklock, N. W. Shworak, X. Bai, J. D. Esko, G. H. Cohen, R. J. Eisenberg, R. D. Rosenberg, P. G. Spear, *Cell* **1999**, *99*, 13–22.

Manuscript received: July 11, 2023
Accepted manuscript online: August 9, 2023
Version of record online: September 6, 2023